Supplementary information for:

Independent hypothalamic circuits for social and predator fear

Bianca A. Silva, Camilla Mattucci, Piotr Krzywkowski, Emanuele Murana, Anna Illarionova, Valery Grinevich, Newton S. Canteras, Davide Ragozzino, Cornelius T. Gross

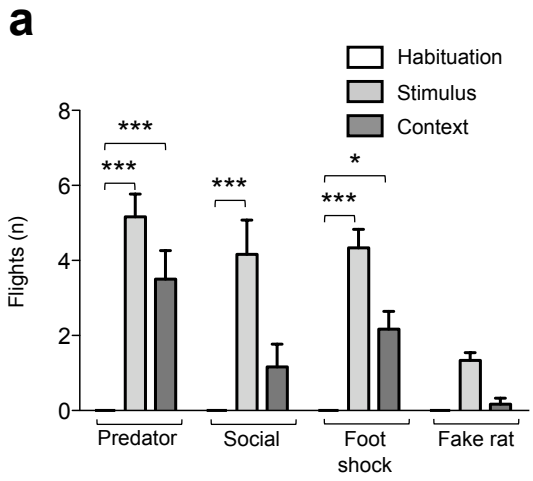

Supplementary Figure 1 (related to Figure 1a-d). Flight behavior elicited in mice by different classes of threat**.** (**a**) The number of flight behaviors performed during the post-stimulus (Stimulus) free exploration period were significantly increased after predator, aggressive conspecific, and foot shock, but not toy rat exposure when compared to the pre-stimulus habituation (Habituation) session. Re-exposure to the context (Context) elicited an increase in flights to predator and foot shock, but not aggressive conspecific or toy rat (Predator: N = 15, Social: N = 9, Foot shock: N = 6, Fake rat: N = 6, * $P < 0.05$, *** $P < 0.001$).

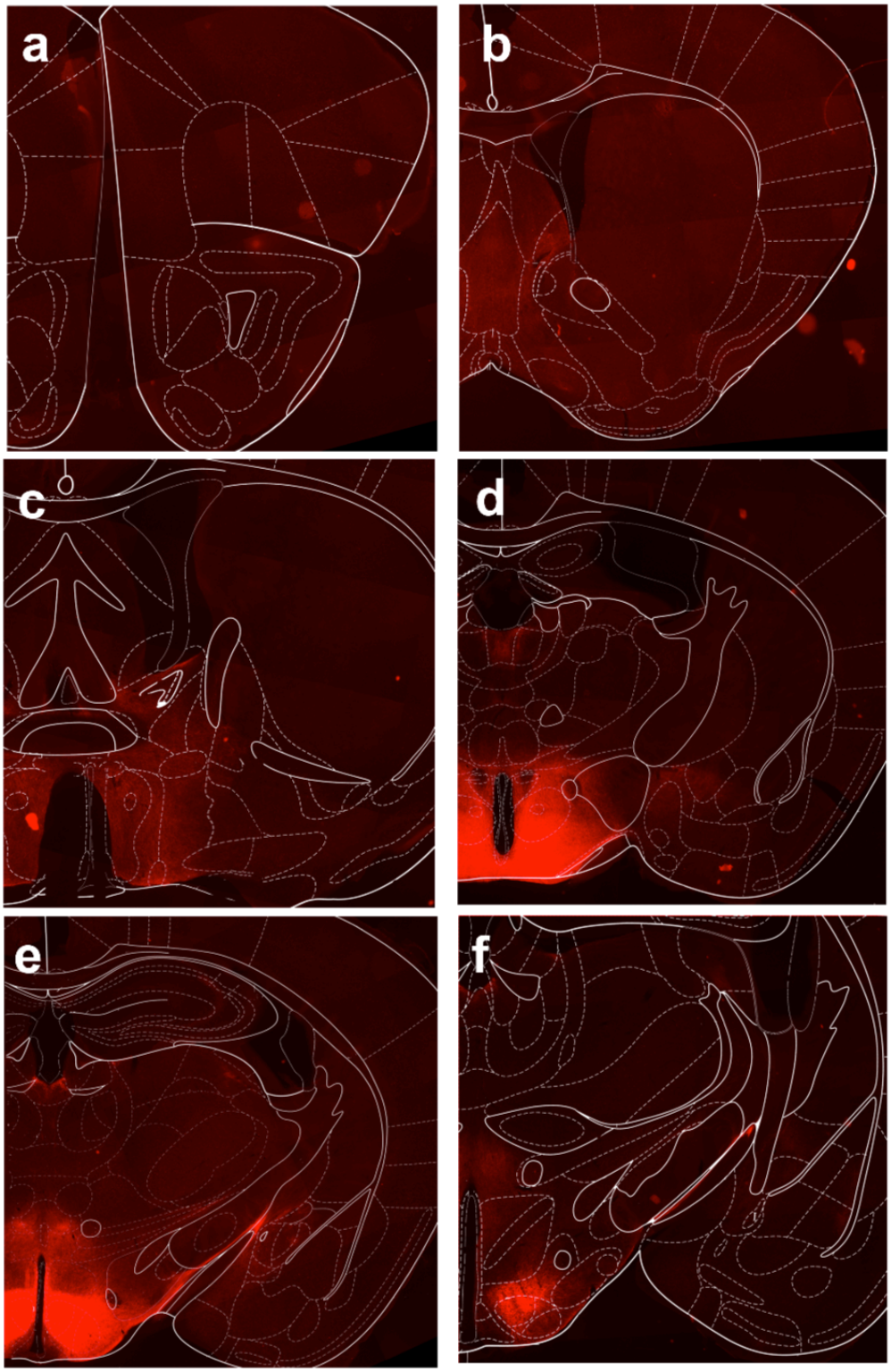

Supplementary Figure 2 (part I).

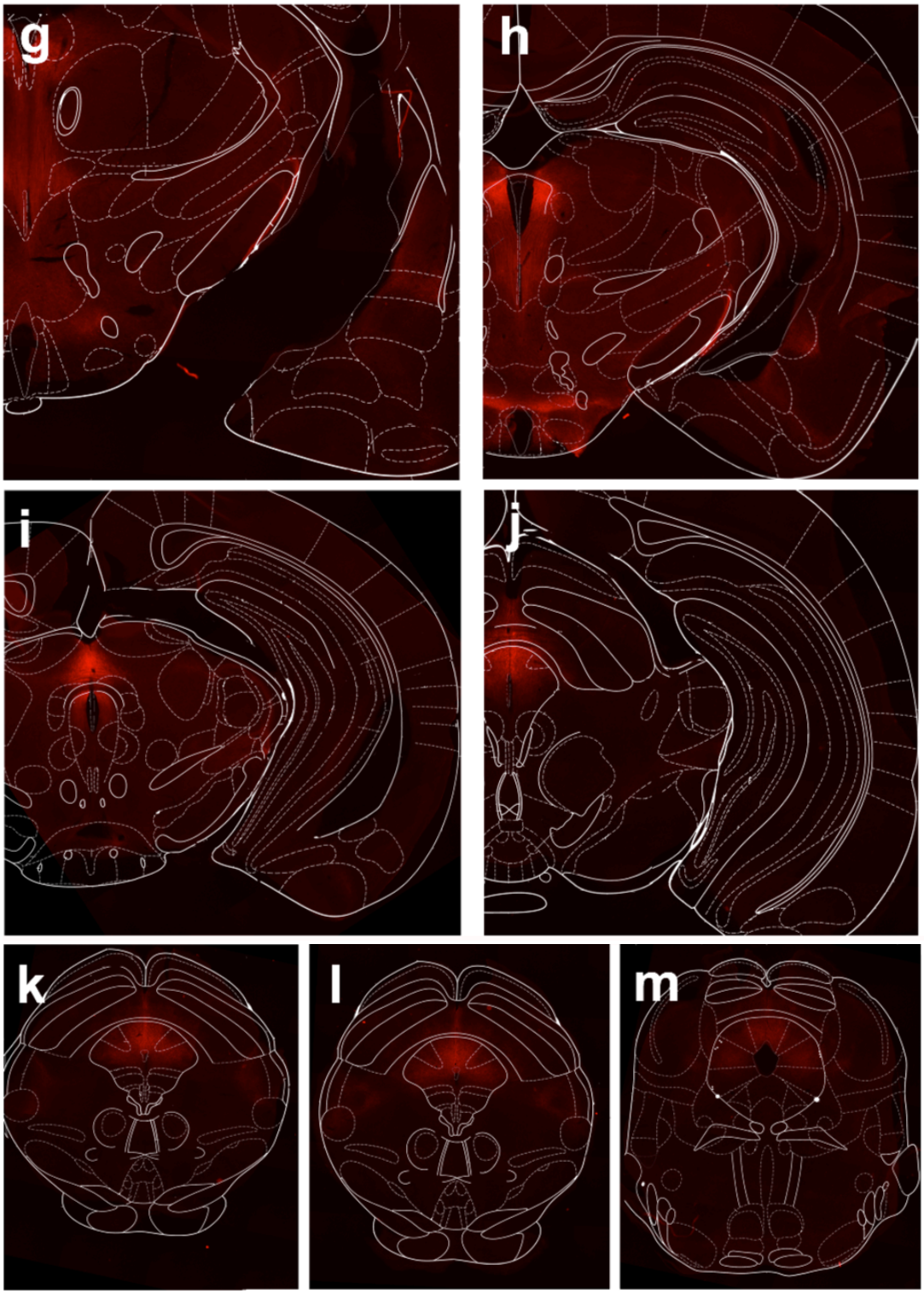

Supplementary Figure 2 (part II).

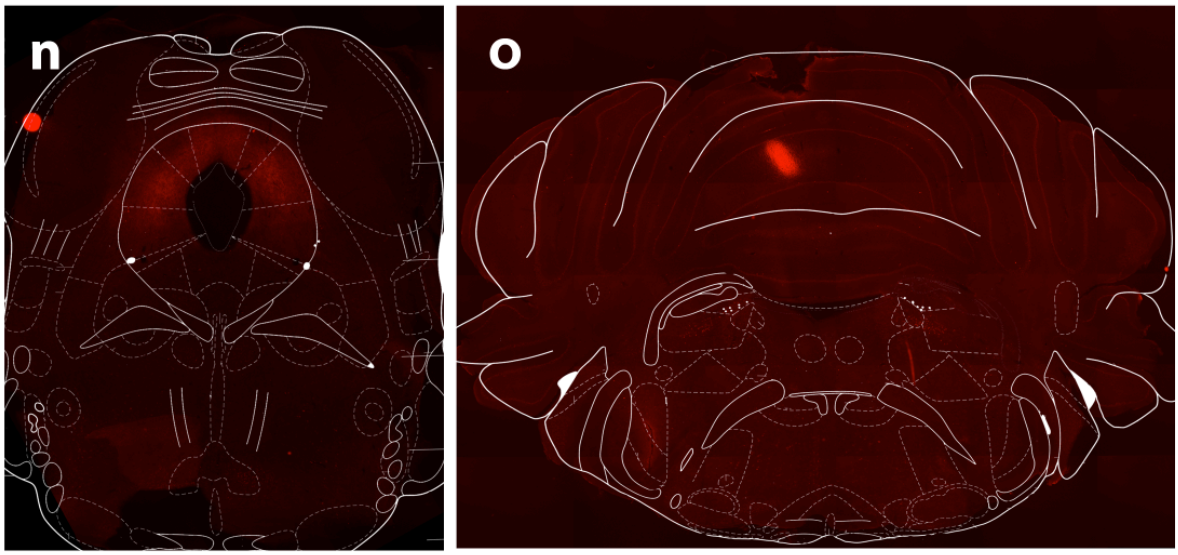

Supplementary Figure 2 (part III) (related to Fig. 2a-d). TomatoF expression in *Nr5a1*::*hM4D*-2A-*tomatoF* transgenic mice. Farnesylated tomato (tom-f, see Fig. 2a) expression was found in cell bodies in the VMHdm and in projections in a number of previously reported target brain regions [10]. Fluorescent images of (**a-o**) rostral to caudal coronal brain sections from *Nr5a1*::*hM4D*-2A-*tomatoF* transgenic mice are shown overlaid with the outlines of mouse brain structures deriving from a standard anatomical atlas [22]. Atlas outlines were morphed in some cases to better match the sections.

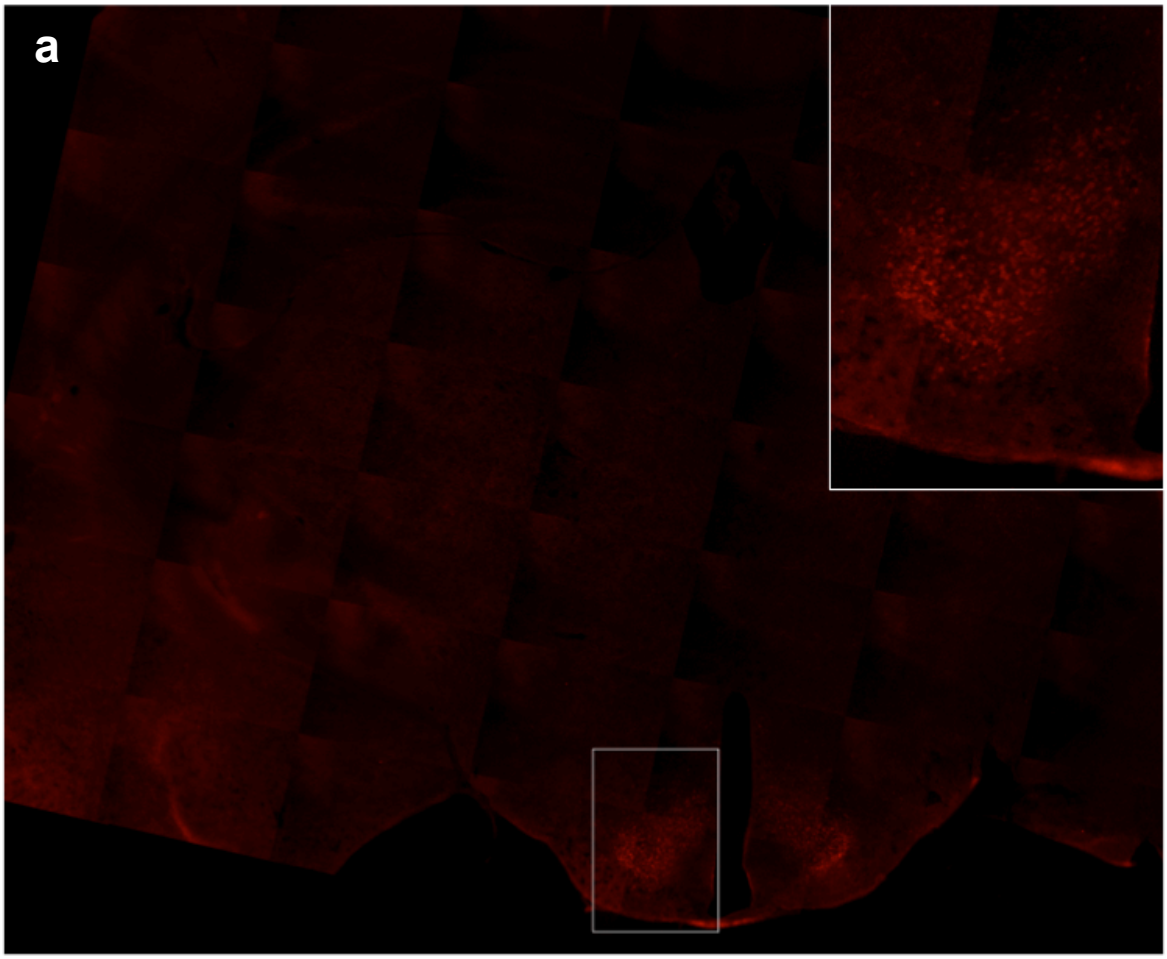

Supplementary Figure 3 (related to Fig. 2f). HA-hM4D is selectively expressed in VMHdm of *Nr5a1*::*hM4D*-2A-*tomatoF* mice. (**a**) Immunofluorecence with anti-HA antibodies in coronal brain sections of *Nr5a1*::*hM4D*-2A-*tomatoF* transgenic mice revealed robust expression of HA-hM4D in the dorsal-medial and central portions of VMH. No detectable anti-HA staining was seen outside VMH.

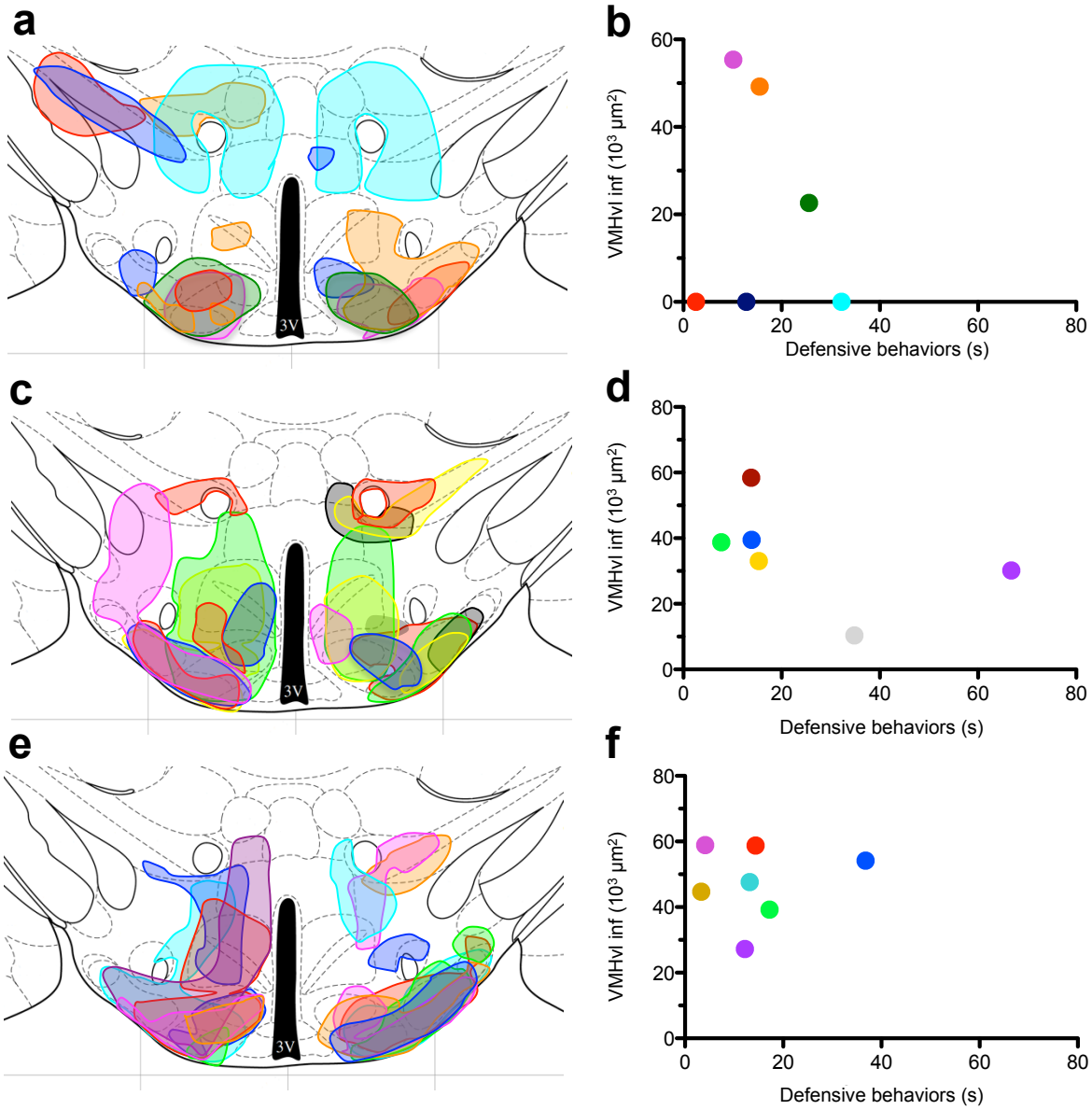

Supplementary Figure 4 (related to Fig. 3e-f). Extent of infection and its correlation with defensive behavior in mice locally injected with AAV-*Syn*::*Venus*-2A-*hM4D* in VMHvl. (**a**, **c**, **e**) Diagrams and (**b**, **d**, **f**) quantitative graphs of the extent of infection as estimated by Venus reporter gene expression in individuals from three groups (**ab**, **cd**, **ef**) of mice injected locally with AAV-*Syn*::*Venus*-2A-hM4D in the VMHvl and treated with CNO. Diagrams show the color-coded extent of infection superimposed on a coronal brain section from a standard atlas [22] (Bregma -1.82). Graphs show the total area of bilateral infection in posterior VMHvl (color-coding matches diagrams) plotted against the defensive behavior displayed by CNO treated animals in response to exposure to an aggressive conspecific.

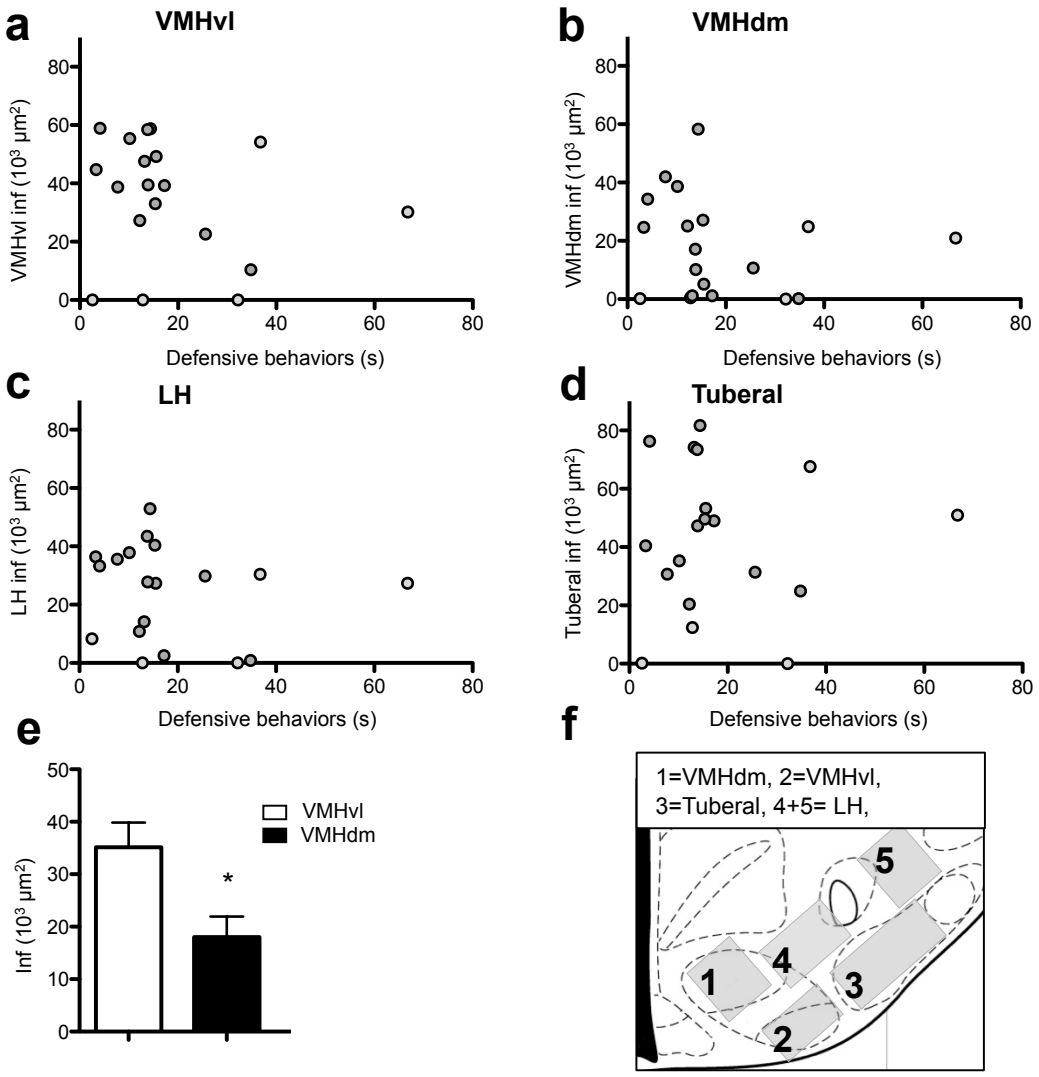

Supplementary Figure 5 (related to Fig. 3d-e). Correlation of extent of infection in different hypothalamic areas and defensive behaviors in mice locally injected with AAV-*Syn*::*Venus*-2A-*hM4D* in VMHvl. Extent of infection (total bilateral area) in (**a**) VMHvl, (**b**) VMHdm, (**c**) lateral hypothalamus (LH), and (**d**) tuberal nucleus plotted against the amount of defensive behaviors displayed by CNO treated animals in response to exposure to an aggressive conspecific. Correlation between the extent of infection and defensive behavior was calculated by MANCOVA ($P = 0.032$) followed by pairwise correlations with VMHvl (Pearson's $r = -0.708$, $P < 0.01$), VMHdm (Pearson's $r = -0.524$, $P > 0.05$), LH (Pearson's $r = -0.482$, $P > 0.05$), and tuberal (Pearson's $r = -0.315$, $P > 0.05$) nuclei. For the statistical analysis outliers (reported in lighter grey) showing poor infection (< 20,000 µm² total infection, N = 3) or behavior (> 1.5 x IQR above third quartile, N = 2) were excluded.

(**e**) A significantly lower extent of infection was seen in VMHdm compared to VMHvl in these animals (N =19, * $P < 0.05$). (**f**) Scheme of the areas used for quantification of each region. Rectangular areas were matched on nuclei from a standard atlas [22]. For quantification in the tuberal nucleus we considered the area located in the base of the tuberal region of the hypothalamus, just laterally to the VMHvl as described by [10].

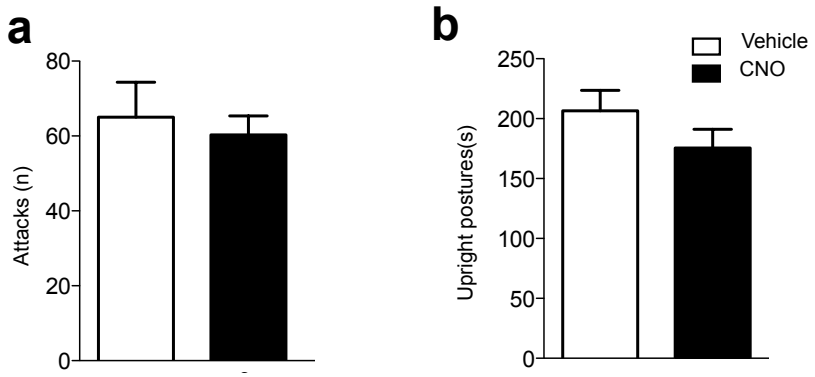

Supplementary Figure 6 (related to Fig. 3d-f). Attacks received and submissive behavior were not affected by pharmacogenetic inhibition of VMHvl. Number of (**b**) upright postures or (**a**) biting attacks received by the experimental mouse infected in VMHvl with AAV-*Syn*::*Venus*-2A-*hM4D* during the encounter with the aggressive stimulus mouse was not altered by CNO treatment when compared to vehicle treated control mice (VMHvl: N = 17-19, $P > 0.05$).

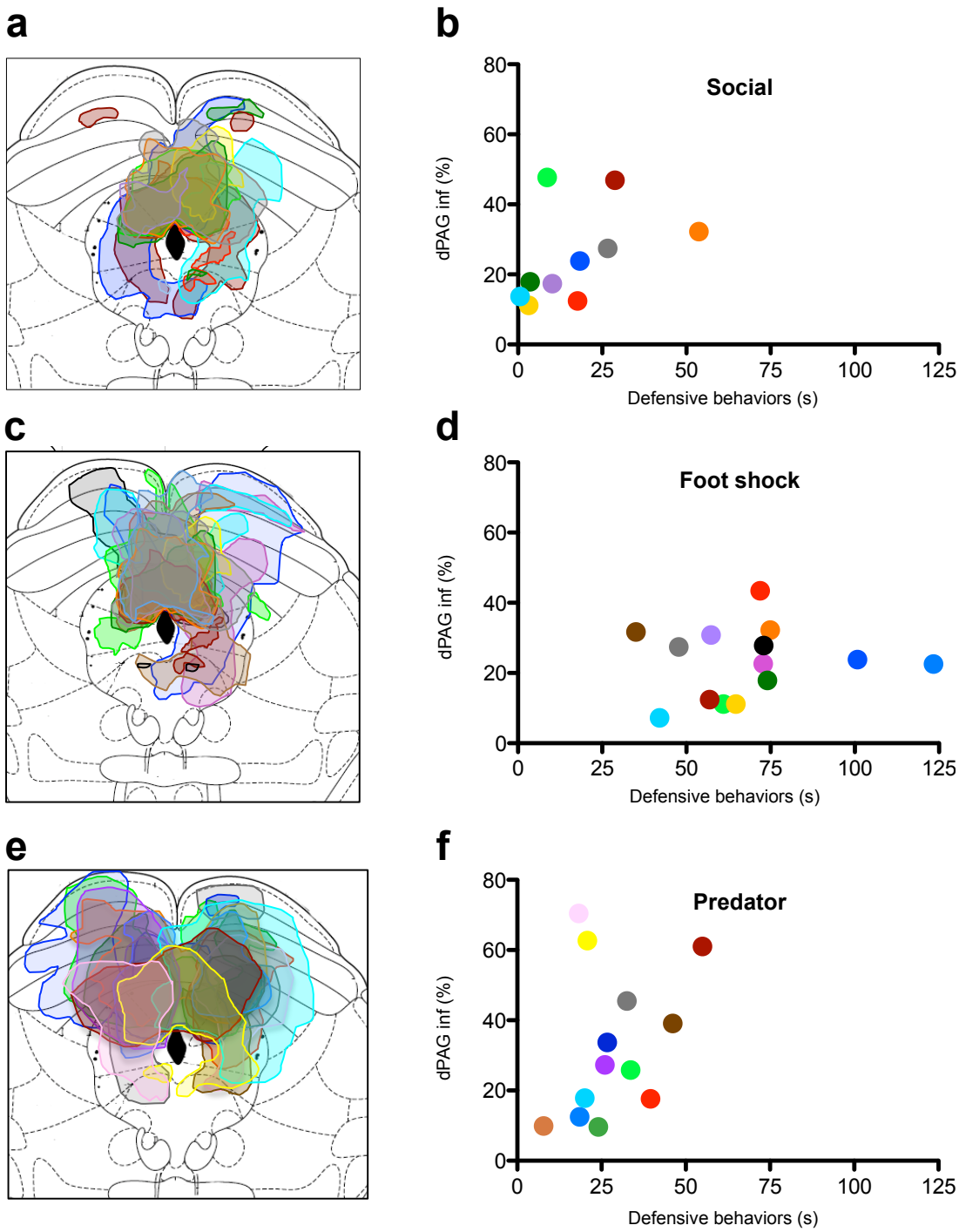

Supplementary Figure 7 (related to Fig. 3g-h). Extent of infection and its correlation with defensive behavior in mice locally injected with AAV-*Syn*::*Venus*-2A-*hM4D* in dPAG.

(**a**, **c**, **e**) Diagrams and (**b**, **d**, **f**) quantitative graphs of the extent of infection as estimated by Venus reporter gene expression in mice injected locally with AAV-*Syn*::*Venus*-2A-*hM4D* in the dPAG and treated with CNO. Diagrams show the color-coded extent of infection superimposed on a coronal brain section from a standard atlas [22] (Bregma -4.36). Graphs show the average percentage of bilateral infection in dPAG (color-coding matches diagrams) plotted against the defensive behavior displayed by CNO-treated animals in response to exposure to an aggressive conspecific (**ab**, Social; **cd**, Foot shock; **ef**, predator).

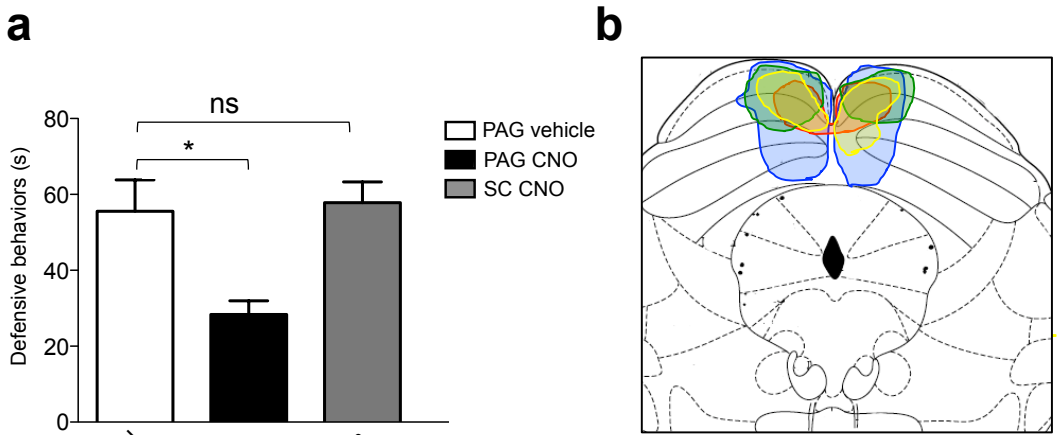

Supplementary Figure 8 (related to Fig. 3g-h). Mice injected with AAV-*Syn*::*Venus*-2A-*hM4D* in superior colliculus (SC) and treated with CNO do not show decreased defensive behavior to a predatory rat. (**a**) CNO-treated mice locally injected with AAV-*Syn*::*Venus*-2A-*hM4D* in dPAG (N = 13, $P < 0.05$), but not SC (N = 4, $P > 0.05$) showed a decrease in defensive behaviors to a predatory rat compared to similarly infected vehicle-treated mice (N = 5). (**b**) Diagram showing the extent of infection superimposed on a coronal brain section from a standard atlas [22] (Bregma -4.36) in individual CNO-treated mice injected with AAV-*Syn*::*Venus*-2A-*hM4D* in SC.

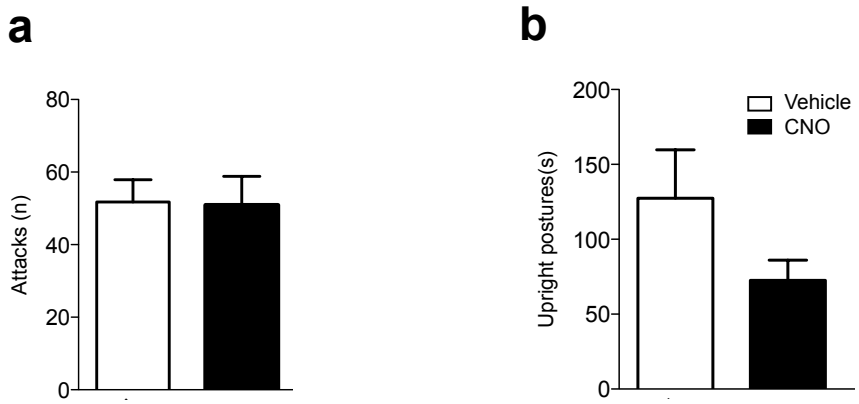

Supplementary Figure 9 (related to Fig. 3g-h). Attacks received and submissive behaviors following pharmacogenetic inhibition of dPAG. CNO treatment did not change the (**a**) number of attacks received by mice infected in dPAG with AAV-*Syn*::*Venus*-2A-*hM4D*. (**b**) Time spent in upright postures during the encounter with the aggressive stimulus mouse was decreased by CNO treatment when compared to vehicle treated control mice (N = 9-10).